were not able to separate the parentages of multiply occurring terms. The formulae derived above overcome this difficulty.

Kronig strengths for a great number of transitions were calculated by Goldberg.[20] His tables have to be multiplied by suitable factors to comply with the normalization adopted above.[21] From the Kronig strengths for $d^2s\cdot p-d^2s\cdot d$ and the parentages of Tables XIV–XVI we then obtain the multiplet strengths for $d^2s\cdot p$–$d^3\cdot s$ as listed in Tables VIII, X, and XII, column 1. When these values are summed over the multiply-occurring terms of both configurations one obtains the multiplet strengths listed by Goldberg.[20]

In the same fashion other tables of multiplet strength relevant to Ti *I* are calculated and are given in Tables IX–XIII, column 1.

[20] L. Goldberg, Astrophys. J. **82**, 1 (1935).
[21] L. Goldberg, Astrophys. J. **84**, 11 (1936).

PHYSICAL REVIEW VOLUME 74, NUMBER 10 NOVEMBER 15, 1948

The Zeeman Effect in Microwave Molecular Spectra*

C. K. JEN
Cruft Laboratory, Harvard University, Cambridge, Massachusetts
(Received July 26, 1948)

A microwave cavity spectroscope is described, which possesses a high sensitivity and resolution for the observation of the Zeeman effect of molecular absorption lines in the microwave frequency range. The theory of operation for this spectroscope and the criteria for sensitivity are formulated.

The Zeeman effect of a number of microwave spectral lines has been measured for the gas molecules $N^{14}H_3$, $N^{15}H_3$, and CH_3Cl^{35} and observed for CH_3Cl^{37} and SO_2. All the experimental results obtained so far can be satisfactorily explained by the combined magnetic contribution due to nuclear and molecular g factors, if there exists a spin-rotation coupling, or solely by the magnetic contribution due to molecular rotation, if there is no such coupling. Thus, further knowledge of the nuclear and molecular magnetic properties of molecules can be obtained through the examination of the Zeeman effect in microwave absorption spectra.

I. INTRODUCTION

THROUGHOUT the history of atomic spectra, the study of the Zeeman effect has provided an exceedingly powerful tool in elucidating the mechanism of the emission and absorption of radiation energy. It gave a great impetus to the early electron theory by emphasizing the important role of the electron in the radiation process. It laid a physical basis for the theory of space quantization, which is an important feature of the quantum theory. Then, the unassailable evidence of the "anomalous" Zeeman effect which had puzzled physicists for a quarter of a century finally led, together with the phenomenon of multiplet structure, to the introduction of the electron spin hypothesis. It soon became clear that an analogous situation existed in the atomic hyperfine structure, where the nuclear spin played a role similar to that of the electron spin in the atomic fine structure. The Zeeman effect became again instrumental in clarifying the situation through the effect of the magnetic moment, associated with the nuclear spin, in an external magnetic field.

The advent of microwave techniques in recent years has given rise to a new branch of spectroscopy. It has been found that a microwave system used as a spectroscopic instrument is capable of a very high resolving power, essentially because the frequency is directly measurable. Such a property can be used to great advantage for investigating the Zeeman effect, since measurements are possible with hyperfine line splittings in a fairly weak magnetic field,

* The research reported in this document was made possible through support extended Cruft Laboratory, Harvard University, jointly by the Navy Department (Office of Naval Research) and the Signal Corps, U. S. Army, under Contract N5ori-76, T. O. 1.

whereas similar measurements in optical atomic spectra would require enormously high fields. Moreover, the fact that microwave frequencies fall mostly in the range of molecular rotational frequencies means that some of the molecular properties can also be studied through the Zeeman effect.

II. A MICROWAVE CAVITY SPECTROSCOPE

There are essentially two requirements that must be satisfied for a microwave spectroscope to be used in connection with experiments on the Zeeman effect. First, the spectroscope must fulfill the usual function of exhibiting the intensity of a spectral line as a function of frequency. In so doing, it must possess the desired degree of sensitivity and resolving power. Second, a magnetic field of sufficient strength and uniformity must be applied to the absorbing specimen. A consideration of these requirements has led to the adoption of a resonant cavity as the absorption cell in the present experiment.

A. Theory of a Gas-Filled Resonant Cavity

The resonant property of a cavity may be characterized by a loss factor δ, which is the ratio of the energy lost per radian to the stored energy, and a resonant frequency ν_0. If there is only one coupling hole between the cavity and a wave guide as in the case of a reflection cavity, then the reflection factor Γ_0 of an empty cavity,[1] defined as the ratio of the complex amplitude of the reflected wave to that of the incident wave, is, for the case $\nu \doteq \nu_0$,

$$\Gamma_0 = \frac{2\delta_1}{\delta_1+\delta_0+i2[(\nu-\nu_0)/\nu_0]} - 1, \qquad (1)$$

where δ_0 = δ-factor due to energy loss in the cavity wall, δ_1 = δ-factor due to energy loss through the window, ν = frequency of the incident wave, ν_0 = resonant frequency of the empty cavity, and $i=(-1)^{\frac{1}{2}}$. If the cavity is now filled with a low pressure gas, then the reflection factor Γ_g would be the same as in Eq. (1), except that ν_0 should now be replaced by $\nu_0/(\epsilon)^{\frac{1}{2}}$, where $\epsilon=\epsilon'-i\epsilon''$, the complex dielectric constant of the gas. In the case of resonance absorption, the real and imaginary parts of ϵ are given as follows[2] ($\nu \doteq \nu_g$):

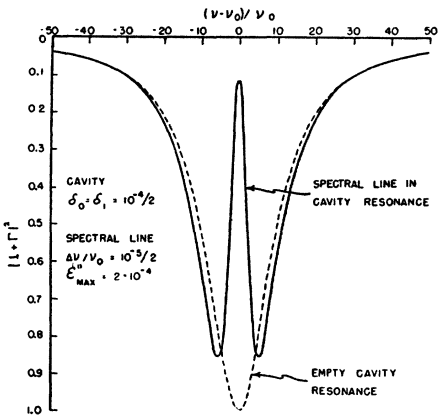

FIG. 1. Theoretical curve of a spectral line in cavity resonance.

$$\epsilon' = 1+(A\nu_g/2)[(\nu_g-\nu)/((\Delta\nu)^2+(\nu-\nu_g)^2)], \qquad (2)$$

$$\epsilon'' = (A\nu_g/2)[\Delta\nu/((\Delta\nu)^2+(\nu-\nu_g)^2)], \qquad (3)$$

where ν_g = resonant frequency of a gas molecule, $\Delta\nu$ = "half-breadth" of a spectral line, A = dimensionless constant dependent on the nature of gas, pressure, temperature, etc. We can assume for most gases at a low pressure $\epsilon'' \ll \epsilon' \doteq 1$. Hence, the reflection factor Γ_g for a gas-filled cavity is

$$\Gamma_g = \frac{2\delta_1}{\delta_1+\delta_0+\epsilon''+i2[((\epsilon')^{\frac{1}{2}}\nu-\nu_0)/\nu_0]} - 1. \qquad (4)$$

It may be seen from Eq. (1) that $|1+\Gamma_0|^2$ as a function of ν is representable by a simple resonance curve, while Eq. (4) indicates that $|1+\Gamma_g|^2$ is representable by a "double-hump" resonance curve with a dip in the middle, if $\nu_g=\nu_0$ and $\Delta\nu/\nu_g \ll (\delta_1+\delta_0)/2$ (i.e., the spectral line breadth is much narrower than the breadth of the cavity response curve). A spectral line can thus be shown in the midst of a cavity resonance curve, as illustrated in Fig. 1.

B. Spectroscopic Sensitivity

As a measure of the spectroscopic sensitivity, the minimum detectable absorption coefficient will now be derived. The largest change of the reflection factor resulting from the introduction

[1] C. K. Jen. J. App. Phys. **19**, 649 (1948).

[2] P. Debye, *Polar Molecules* (Reinhold Publishing Corporation, New York, 1929), Chap. V.

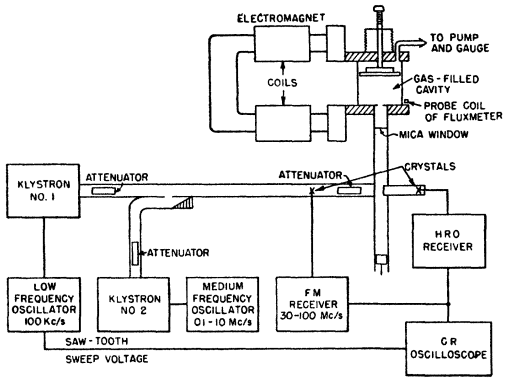

FIG. 2. A schematic diagram of the complete system for measurements of microwave Zeeman spectra.

of the absorbing gas occurs at $\nu=\nu_0=\nu_g$. Let V_0 represent the voltage amplitude of the incident wave, then the change in voltage caused by resonance absorption is, according to Eqs. (1) and (4), with $\epsilon''\ll\delta_1+\delta_0$,

$$\Delta V=V_0(\Gamma_0-\Gamma_g)_{\nu=\nu_0=\nu_g}=[2\delta_1/(\delta_1+\delta_0)^2]\epsilon''V_0. \quad (5)$$

Maximizing ΔV relative to the parameter δ_1 leads to the condition $\delta_1=\delta_0$. Let $\delta_1+\delta_0=\delta=1/Q$, where Q is the "loaded" Q factor of the cavity, then the maximum value of ΔV is

$$(\Delta V)_{\max}=Q\epsilon''V_0. \quad (6)$$

For minimum detectability, this voltage should be equated[3] to the r.m.s. voltage associated with thermal noise $(\overline{V_n^2})^{\frac{1}{2}}=(4kTN\Delta fZ_0)^{\frac{1}{2}}$, where k=Boltzmann's constant, T=absolute temperature, N="noise figure," Δf=band width of the receiver, and Z_0=characteristic impedance of the wave guide. Using the usual relation $\alpha=(2\pi/\lambda)(\epsilon''/(\epsilon')^{\frac{1}{2}})\doteq(2\pi/\lambda)\epsilon''$, where α=absorpsion coefficient due to gas and λ=free space wave-length, we have for the minimum detectable α

$$(\alpha)_{\min}=(4kTN\Delta f/P_0)^{\frac{1}{2}}(2\pi/Q\lambda), \quad (7)$$

in which $P_0=V_0^2/Z_0$, the incident power. It is well known that the factor $Q\lambda/2\pi$ in Eq. (7) is the cavity equivalent of the absorption path length in free space. Thus a high Q cavity is required for high spectroscopic sensitivity.

As a numerical example, assume $T=293°$K, $Q=10^4$, $\lambda=1.25$ cm, and the following two cases: (a) $N=100$, $\Delta f=3000$ c.p.s., $P_3=10^{-4}$w, then $(\alpha)_{\min}=0.35\times10^{-8}$ cm^{-1}; (b) $N=31.6$, $\Delta f=30$ c.p.s., $P_0=10^{-3}$w, then $(\alpha)_{\min}=0.62\times10^{-10}$ cm^{-1}. Case (a) represents very nearly the condition of the present experiment, while case (b) may perhaps be achievable with further improvement of technique.

[3] R. V. Pound, Proc. I.R.E. **35**, 1414 (1947).

C. Cavity Design

It was shown in Eq. (7) that for use in a sensitive spectroscope, a cavity must possess a high Q-factor, while maintaining the condition of "match," $\delta_1=\delta_0$. Yet, this Q-factor should be smaller (e.g., ten times) than what might be described as the Q-factor of a spectral line, $\nu/2\Delta\nu$. This latter condition is to allow almost the whole of a spectral line to be well within the most sensitive portion of the cavity resonance.[4] Thus, for a microwave frequency ν of about 24,000 Mc/sec. in the K-band, and a spectral line breadth $\Delta\nu$ of about 0.12 Mc/sec., then the cavity Q-factor should be of the order of 10^4. A cavity with this Q would be equivalent to about 20 meters of absorption path and would have the sensitivity mentioned in the preceding section. However, it has been found difficult to attain such a Q-factor, with the linear dimensions of the cavity comparable to one-half of the wavelength in the cavity. One should therefore use the resonances occurring at higher modes in a larger cavity, since the Q-value of such a cavity would increase almost in proportion with the linear dimensions. A larger cavity is also more favorable from the standpoint of "intensity saturation" of spectral lines (cf. the following section).

In view of the above discussion, we have adopted for use in our K-band spectroscope a cylindrical cavity of the size ordinarily used as an X-band wave meter. This cavity has an inner diameter of 4.952 cm and a tunable length roughly 2.1 to 3.4 cm. At any particular frequency, the cavity can be tuned to any one of approximately twenty modes which have Q-values varying from twice 10^4 to many times less. This situation is conveniently adaptable to meeting various requirements of observation.

[4] The other alternative is to make $Q\gg\nu/2\Delta\nu$ and thus "trace out" a spectral line with the cavity resonance. This will call for exceedingly high cavity Q-factors for narrow spectral lines.

For the study of the Zeeman effect, the end plates of the cylindrical cavity serve as pole pieces for the electromagnet. They are made of magnetic steel, silver-plated on the inside to maintain high conductivity. In terms of the classical Zeeman effect, one observes the π-components, when the microwave electric field is parallel to the steady (axial, in this case) magnetic field, or the σ-components when the two fields are perpendicular.

D. Microwave Circuit

The choice of the microwave circuit, together with the methods of modulation, detection, and amplification, should be consistent with the implications contained in Eq. (7). The objective is obviously to keep the factor $N\Delta f/P_0$ as low as possible for high sensitivity. There is, however, an upper limit for the incident power on account of the effect of "intensity saturation." This means that the gas absorption coefficient will drop and the spectral line will broaden, if P_0 exceeds a limiting value, which is essentially a direct function of the total number of absorbing gas molecules. With a given cavity size and an operating pressure, which determines a desired line breadth, the limiting incident power is a well defined quantity. The noise figure is a result of random disturbances from many sources: klystron, crystal detector, amplifier, etc. It is currently believed that a major portion of this noise, particularly that arising from the crystal detector, is an inverse function of frequency. This suggests the desirability of using a modulation technique so that the signal can be detected and amplified at an intermediate frequency. The band width Δf should be narrow to minimize noise, but, if we are going to use a frequency modulation such as that produced by a saw-tooth voltage on the repeller plate of the klystron, Δf has to be wide enough to secure a complete representation of a spectral line. Let D = maximum microwave frequency displacement caused by a modulation voltage, f_s = repetition or sweep rate of the frequency modulation, n = a number large enough to include many Fourier harmonic terms for accurate representation of the spectral line, and $\Delta\nu$ = half-breadth of the spectral line; then we can derive the following expression

$$f_s = \Delta f \Delta\nu / nD. \tag{8}$$

Eq. (8) shows that, for a given $\Delta\nu$, the quantity f_sD must be kept low enough as to achieve a satisfactorily small Δf.

Figure 2 gives a complete schematic diagram of the microwave circuit adopted for the present experiment, including arrangements for the magnetic field and measurement of frequency differences to be discussed later. Klystron No. 1 (a 2K33 tube) sends a radiation along a K-band wave guide through two attenuators. The wave splits into two components at the "magic tee," one going toward the resonant cavity and the other toward the tuning plunger. The vector difference of the two reflected waves will go through the E-plane arm of the magic tee and finally to the crystal. If the two wave guide arms are exactly equal, the amplitude of the voltage received at the output crystal, V_R, is then

$$V_R = (|1+\Gamma|/2)\, V_0, \tag{9}$$

which shows that we now have an experimental representation of the factor $|1+\Gamma|$, already theoretically discussed in Eqs. (1) and (4).

Since it has been shown above that crystal detection is more favorable at an intermediate frequency from the point of view of low noise figure, we have adopted a frequency-modulation scheme first suggested by Hershberger.[5] The repeller plate of the Klystron is modulated by a sinusoidal voltage with a frequency around 100 kc, in addition to the saw-tooth voltage sweep. Reception at this frequency or a higher harmonic is, in this instance, accomplished by an HRO

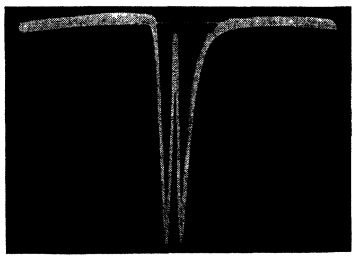

FIG. 3. Oscilloscopic pattern for a spectral line in cavity resonance.

[5] At the Symposium on Molecular Structure and Spectroscopy, Ohio State University, Columbus, Ohio (June 9–14, 1947).

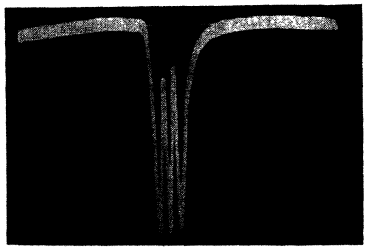

FIG. 4. Zeeman splitting of a spectral line in cavity resonance at $H=700$ oersteds.

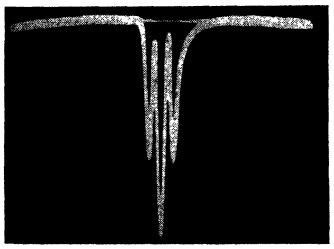

FIG. 5. Zeeman splitting of a spectral line in cavity resonance at $H=1200$ oersteds.

receiver, and the output is applied to the vertical plates of an oscilloscope. The horizontal plates of the oscilloscope are driven by the same saw-tooth voltage that sweeps the klystron at a rate of about 20 c.p.s. Some characteristics of this system are typified by the numerical example in case (a) in Section B of Part II.

Figure 3 is an experimental curve for a spectral line ($N^{14}H_3$)($JK=88$) in the middle of a cavity resonance curve (at a pressure of about 10^{-2} mm Hg), a verification of the theory illustrated in Fig. 1.

E. Zeeman Splitting and Frequency Measurement

The Zeeman effect of the microwave spectral lines can now be very readily studied by applying an axial magnetic field as shown in Fig. 2. Only a weak field, continuously variable from 0 up to 1670 oersteds, has been used thus far in this experiment. The field strength is measured by means of a small search coil connected in series with a Rawson fluxmeter, and the mean field inside the cavity is estimated from the results of probing another similar but cut-away cavity. The maximum non-uniformity of field has been found to be about four percent from the mean value.

Figure 4 shows a typical Zeeman doublet pattern for the $N^{14}H_3$ $JK=88$ line in a field of about 700 oersteds, and Fig. 5 shows the splitting at about 1200 oersteds. The spectral resolution is partly limited by the natural breadth of the spectral line and partly by the non-uniformity of the magnetic field. The limit of resolution for the present apparatus is roughly of the order of 250 kc.

The method of measuring frequency differences for the Zeeman splitting is also shown in Fig. 2. The radiation from Klystron No. 2 forms a variable beat frequency with that of Klystron No. 1, which is being linearly swept, as a result of the mixer action of the crystal situated just before the second attenuator. The f-m receiver selects a beat frequency that is coincident with its own tuning and presents a pip on the scope. If frequency modulation is applied to Klystron No. 2, then there is an evenly spaced line spectrum on each side of the pip, with the spacing between any two adjacent lines equal to the modulation frequency itself. Thus the difference frequency between any two Zeeman components can be measured by matching the variable measuring pips to the Zeeman components. This procedure is shown in Fig. 6.[6]

III. ZEEMAN SPECTRA AND INTERPRETATION

The Zeeman effect in the microwave region was first observed by Coles and Good[7] in the inversion spectrum of ammonia. They applied a magnetic field of 6600 oersteds to a coil of wave guide containing the absorbing gas and found a doublet splitting when the magnetic field was perpendicular to the microwave electric field. No interpretation of the effect was given in their paper.

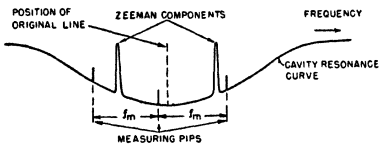

FIG. 6. Measurement of frequency difference for Zeeman splitting.

[6] The use of this modulation spectrum as a frequency-difference indicator instead of the single pip movable with the tuning of the f-m receiver is to obviate any difficulties arising from the inherent instability of the Klystron No. 2.

[7] D. K. Coles and W. E. Good, Phys. Rev. **70**, 979 (1946).

In this paper, the Zeeman effect for the microwave spectra of several gases,[8,9] including $N^{14}H_3$, $N^{15}H_3$, CH_3Cl^{35}, CH_3Cl^{37}, and SO_2 has been investigated, using a resonant cavity as the absorption cell and a weak but perhaps more uniform magnetic field. On the basis of quantitative data obtained for the first three of these gases, satisfactory interpretations of the phenomena can be made in terms of nuclear and molecular magnetic moments, which will be explained in the following sections.

A. Zeeman Spectra of $N^{14}H_3$ Inversion Spectrum

The inversion spectrum of $N^{14}H_3$ has the distinction of being historically the first and so far the most attractive subject of investigation in microwave spectroscopy. In particular, it was in this spectrum that the hyperfine structure of a microwave spectral line was first discovered by Good[10] and later successfully explained by Van Vleck and his collaborators[11] and by Coles and Good[7] in terms of the nuclear quadrupole moment coupling. More recently, Hendersen and Van Vleck[12] have introduced an additional coupling term due to the nuclear magnetic moment interacting with the magnetic field set up by the molecular rotation. This term, though smaller than that of the nuclear quadrupole coupling, appears to be a necessary inclusion for closer agreement with experiment.

To study the Zeeman effect of this spectrum, we have here applied a magnetic field perpendicular to the microwave electric field for a TE-mode in the cavity. It was found that each line in the hyperfine structure was split in the manner

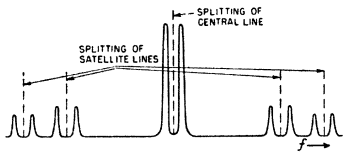

FIG. 7. Zeeman splitting of an $N^{14}H_3$ line and its satellite lines.

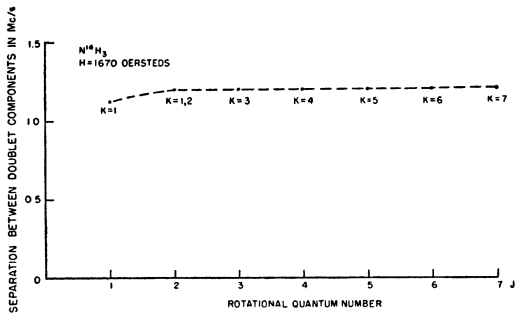

FIG. 8. Zeeman splitting of $N^{14}H_3$ inversion lines.

shown in Fig. 4 or 5. Figure 7 shows the Zeeman pattern for each group of such lines characterized by the same JK value (J=quantum number of the total angular momentum, and K=quantum number of the component of the angular momentum about the figure axis). It is seen that each line is split into a doublet. Measurements have further shown that the doublet separation is essentially the same for the central line as for any one of the satellite lines.

When the Zeeman effect of the central line is studied at a constant magnetic field from one JK line to another, it was found that the doublet separation is approximately independent of the quantum numbers (see Fig. 8).

The variation in the doublet separation as a function of the magnetic field follows very nearly a linear relationship. A typical curve is shown in Fig. 9 for the $JK=33$ line, with the result $2\Delta\nu/\Delta H=0.718$ Mc/sec. per 1000 oersteds. It is evident, therefore, that we are dealing with a first-order Zeeman effect.

B. Discussion of the $N^{14}H_3$ Zeeman Spectrum

The standard interpretation of the Zeeman effect is based upon the existence of a permanent magnetic moment along the direction of the magnetic field. For the first-order Zeeman effect, the frequency separation between the Zeeman components is proportional to the magnetic field and another factor which is related to the permanent magnetic moment. Thus we may have

$$\Delta\nu=g(\mu_0/h)H, \tag{10}$$

where $\Delta\nu$=difference between the frequency of a Zeeman component and that of the undisplaced line ($\frac{1}{2}$ of the frequency separation between

[8] C. K. Jen, Phys. Rev. **72**, 956 (1947).
[9] C. K. Jen, Bull. Am. Phys. Soc. **23**, May; No. 3 (April, 1948); Phys. Rev. **73**, 1237 (1948).
[10] W. E. Good, Phys. Rev. **70**, 213 (1946).
[11] B. P. Dailey, R. L. Kyhl, M. W. P. Strandberg, J. H. Van Vleck, and E. B. Wilson, Jr., Phys. Rev. **70**, 984 (1946).
[12] R. S. Hendersen and J. H. Vleck, Phys. Rev. **74**, 106–107 (1948).

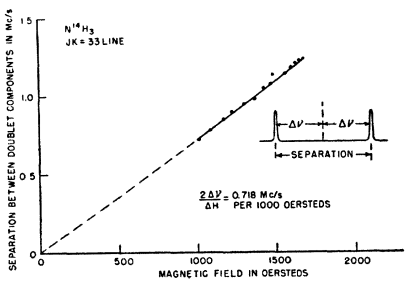

FIG. 9. Zeeman splitting of an $N^{14}H_3$ line as a function of the magnetic field.

two symmetric doublet components), μ_0 = nuclear magneton $= eh/4\pi Mc$, M = proton mass, h = Planck's constant, and g = gyromagnetic ratio or the g-factor. We see from Eq. (10) that the experimental result for a given Zeeman splitting may be concisely stated in terms of the corresponding g-factor. Referring to Figs. 8 and 9, the g-factor for most of the $N^{14}H_3$ lines is of the order of 0.47. It follows that any plausible interpretation of the Zeeman spectra for $N^{14}H_3$ must be able to account for the correct magnitude of the g-factor, the doublet structure of the Zeeman pattern and also the approximate independence of this g-factor as a function of the quantum numbers.

There are at least three possible sources of permanent magnetic moments for an $N^{14}H_3$ molecule: the N^{14} nuclear nuclear magnetic moment, the nuclear magnetic moments due to the three H nuclei and the molecular moment due to rotation. The last one is understood here to include all the magnetic contributions due to orbital motion of all nuclei and electrons in the molecule. The contribution due to the three H nuclei may be ruled out, because the g-factor for a proton, about 5.6, is much to high for any agreement with the experimental g-factor, which is approximately ten times smaller.

It is only necessary now to deal with the interactions between the external magnetic field and the two remaining magnetic moments, one due to N^{14} nuclear spin and the other due to molecular rotation. In the absence of an external field, there exists a spin-rotation coupling, as mentioned above, which gives rise to the hyperfine structure. If, in the presence of the field, the Zeeman splitting is less than the hyperfine structure spacing, the spin-rotation coupling is still in effect. Such a field is usually described by the term "weak," a common restriction in the study of the Zeeman effect. However, as the field is raised beyond this range, the spin-rotation coupling begins to break down gradually, until the field is strong enough to break up the coupling completely (Paschen-Back effect). In the following, a general theory of the Zeeman effect will be developed for the coupling between the spin of a single nucleus and molecular rotation.

C. Theory of Zeeman Splitting for Spin-Rotation Coupling

When the Zeeman effect is smaller than the spin-rotation interaction, we can start with the unperturbed Hamiltonian $\mathcal{H}_0$ describable by a diagonal matrix in the system of representation labeled by $JIFM$, where J = angular momentum quantum number of the molecule, I = nuclear spin quantum number, $F = J+I, J+I-1, ---, J-I+1, J-I$, and $M = F, F-1, ---, -F+1, -F$. The eigenvalues of $\mathcal{H}_0$, W_0, are the energy levels of the unperturbed states labeled in the same way, except that the energy is now independent of M (i.e., each JIF state has a $(2F+1)$-fold degeneracy). The total Hamiltonian $\mathcal{H}$, including the interactions of the external field with the nuclear and molecular magnetic moments, is

$$\mathcal{H} = \mathcal{H}_0 - g_{\text{mole}}\mu_0 \mathbf{J}\cdot\mathbf{H} - g_N\mu_0 \mathbf{I}\cdot\mathbf{H}, \qquad (11)$$

where g_{mole} = g-factor of the molecule along J, g_N = g-factor of the nucleus coupled with the molecule, μ_0 = nuclear magneton, $\mathbf{J},\mathbf{I}$ = vector operators of J, I, and H = external magnetic field. The solution for Eq. (11), with the aim of finding its eigenvalues, is almost exactly the same as the case of the Russell-Saunders coupling in atomic spectra. The only essential difference is that while the g-factors for electron spin and orbital motion are definitely related (ratio = 2:1), the g-factors here, g_{mole} and g_N, are not related at all. We can therefore follow the same procedure of solution,[13] while preserving the identities of the g-factors, and arrive at the following results, which can also be obtained from vector

[13] E. U. Condon and G. H. Shortley, *The Theory of Atomic Spectra* (Cambridge University Press, 1935) Chapter XVI.

model considerations.[14]

$$W=W_0(JIF)-M\mu_0H\{\alpha_J g_{\text{mole}}+\alpha_I g_N\}, \quad (12)$$

where

$$\alpha_J=[F(F+1)+J(J+1)-I(I+1)]/2F(F+1)$$

and

$$\alpha_I=[F(F+1)+I(I+1)-J(J+1)]/2F(F+1).$$

It is worth noting that in Eq. (12), if we let $g_t=\alpha_J g_{\text{mole}}+\alpha_I g_N$ we may say g_t is a total g-factor, which is a linear combination of g_{mole} and g_N with the combination coefficients α_J and α_I as functions of the quantum numbers.

The frequency displacement of any Zeeman component relative to the zero-field position of a hyperfine line can be readily calculated from the following

$$\Delta\nu(J_1F_1M_1\rightarrow J_2F_2M_2)=(\mu_0H/h)\{(Mg_t)_2-(Mg_t)_1\}, \quad (13)$$

where the change of quantum numbers has to obey the usual selection rules: $\Delta J=0, \pm1$; $\Delta F=0, \pm1$; $\Delta M=0, \pm1$. It is understood that the nuclear spin remains constant ($\Delta I=0$), and the axial quantum number K suffers no change ($\Delta K=0$) for transitions in linear and symmetric molecules.

The intensity of any Zeeman component can be calculated from the standard formulas used in atomic Zeeman spectra with only slight changes in notation.[13]

D. Interpretation of the $N^{14}H_3$ Zeeman Spectra

For the Zeeman splitting of the $N^{14}H_3$ inversion spectrum, Eq. (13) takes the following form for $\Delta J=0$ and $\Delta M=\pm1$ (σ components, normally observed in this experiment).

(a) Central line Zeeman components ($\Delta F=0$):

$$\Delta\nu_0=\pm\frac{\mu_0H}{h}\left\{\frac{g_{\text{mole}}+g_N}{2}+\frac{J(J+1)-I(I+1)}{F(F+1)}\frac{(g_{\text{mole}}-g_N)}{2}\right\}. \quad (14)$$

(b) Satellite line Zeeman components ($\Delta F=\pm1$) for satellites closer to central line:

$$\Delta\nu_s=\Delta\nu_0+\frac{M\mu_0H}{h}\left(\frac{1}{J+2}-\frac{1}{J}\right)\times\frac{J(J+1)-I(I+1)}{J+1}\frac{(g_{\text{mole}}-g_N)}{2} \quad (15)$$

where $-J\leq M\leq J$, for satellites further from central line:

$$\Delta\nu_s'=\Delta\nu_0+\frac{M\mu_0H}{h}\left(\frac{1}{J+1}-\frac{1}{J-1}\right)\times\frac{J(J+1)-I(I+1)}{J}\frac{(g_{\text{mole}}-g_N)}{2} \quad (16)$$

where $-(J-1)\leq M\leq J-1$. It is commonly accepted that $I(N^{14})=1$, and it follows that $F=J+1, J, J-1$. We note that the theoretical Zeeman pattern may generally be quite complicated and much dependent on the quantum numbers. There is, however, one important special case, namely $J=I$, for which the equations reduce simply to

$$\Delta\nu_0=\Delta\nu_s=\Delta\nu_s'=\pm\frac{\mu_0H}{h}\frac{g_{\text{mole}}+g_N}{2}. \quad (17)$$

This means, for the $JK=11$ line of $N^{14}H_3$, the Zeeman splitting is strictly a doublet and has the same doublet separation for the satellite lines as for the central line. We can thus determine a value for g_{mole} from the expression $(g_{\text{mole}}+g_N)/2=g_{11}$, where g_{11} is the experimental g-value for the $JK=11$ line. Using $g_N(N^{14})=0.403$ from published nuclear resonance data and $g_{11}=0.44$ from the present experiment, we arrive at the result $g_{\text{mole}}(N^{14}H_3)=0.48\pm0.03$,

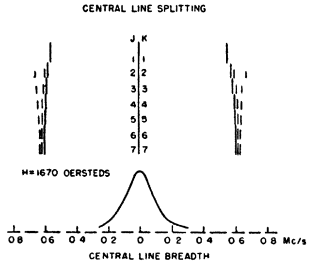

FIG. 10. Calculated Zeeman spectrum for $N^{14}H_3$ lines with $g_N=0.403$ $g_{\text{mole}}=0.48$.

[14] S. Goudsmit and R. F. Bacher, Zeits. f. Physik **66**, 13 (1930).

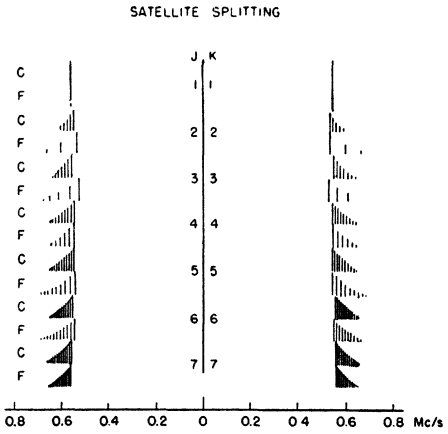

FIG. 11. Calculated Zeeman spectrum for the satellite lines of $N^{14}H_3$ lines with $g_N=0.403$ and $g_{mole}=0.48$ and $H=1670$ oersteds, (*C*) that satellite close to central line, (*F*) that satellite further from central line.

taking into account the inhomogeneity of the magnetic field and other experimental errors.

While g_{mole} may itself depend upon the values of J and K, we can at least temporarily assume that the same g-value holds true for higher JK values and examine the theoretical results from Eqs. (14), (15), and (16). It is clear from these equations that the departure from the strict doublet relationship is proportional to $g_{mole}-g_N$, with the coefficient of proportionality a function of the quantum numbers. However, the fact that g_{mole}, in the case of $N^{14}H_3$, is so close to g_N makes the contribution from the $g_{mole}-g_N$ term sufficiently small so that the experimental Zeeman pattern appears to be a doublet within the limits of resolution and the frequency separation is sensibly independent of the quantum numbers. This statement is well supported by the theoretical results calculated from Eqs. (14), (15), and (16). Figure 10 shows the calculated splittings for the central line bearing various $J=K$ designations and Fig. 11 the same for the satellite lines. It can thus be concluded that within the limits of resolution, the calculated patterns are in good agreement with experiment and that g_{mole} does not depend strongly on the J and K values.

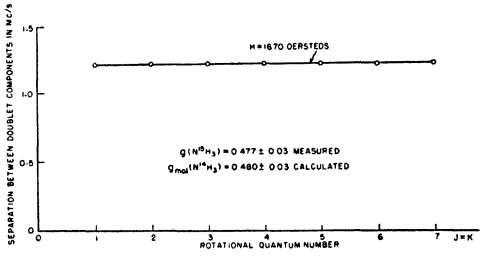

FIG. 12. Zeeman splitting of $N^{15}H_3$ inversion lines.

E. Experimental Results and Interpretation for $N^{15}H_3$ Zeeman Spectra

Since it is known that $I(N^{15})=\frac{1}{2}$, there cannot be any nuclear quadrupole coupling by theory and no trace of hyperfine structure has been found in experiment.[11] The Zeeman splitting in this case should therefore depend exclusively on the molecular g-factor,

$$\Delta\nu=\pm g'_{mole}(\mu_0 H/h), \tag{18}$$

where $g'_{mole}=g_{mole}(N^{15}H_3)$. Now, $g(N^{15}H_3)$ should be slightly less than $g(N^{14}H_3)$ because of the somewhat larger reduced mass resulting from the heavier isotope. A calculation shows, however, that this difference is quite negligible relative to the accuracy of the present experiment. Thus we may take $g(N^{15}H_3)\doteq g(N^{14}H_3)$. This indicates the prospect of verifying the calculated result for $N^{14}H_3$ by the experimental result for $N^{15}H_3$.

Experiments have been performed on the Zeeman splitting of the $N^{15}H_3$ inversion spectrum, following published frequencies.[15] A doublet splitting has been found for all the lines observed in this experiment and the separation is indeed sensibly independent of the quantum numbers for the case $J=K$. Figure 12 shows a plot of these results and also a comparison of the experimental $g(N^{15}H_3)$ with the calculated g_{mole} $(N^{14}H_3)$. The agreement between the two is seen to be quite satisfactory, thus furnishing a further evidence for the interpretation of the $N^{14}H_3$ Zeeman spectra.

F. Zeeman Effect of the Rotational Spectra of CH_3Cl

The Zeeman effect of methyl chloride has been studied because this molecule combines the desirable features of a very strong nuclear quadrupole coupling with the simple structure of a symmetric top. Moreover, its first rotational lines corresponding to $J=0\rightarrow1$ for both CH_3Cl^{35} and

[15] W. E. Good and D. K. Coles, Phys. Rev. **71**, 383 (1947).

CH_3Cl^{37} occur very conveniently near the upper end of the K-band.[16] These lines have been found here in a resonant cavity and their positions determined. Figure 13 shows an energy level diagram including the effects of the nuclear quadrupole coupling and the three possible transitions in zero-field. The nuclear spin I for either Cl^{35} or Cl^{37} has to be 3/2 to get very close agreement with the hyperfine structure. This confirms Townes' assignment for $I(Cl)$ in ClCN.[17] Also, it seems that the nuclear electric quadrupole coupling accounts very accurately for the separation of the energy levels. The theoretical ratio between the frequency difference $\nu(F=3/2\rightarrow 5/2)-\nu(F=3/2\rightarrow 3/2)$ and the frequency difference $\nu(F=3/2\rightarrow 1/2)-\nu(F=3/2\rightarrow 5/2)$ is 1.250, whereas that determined experimentally is 1.252. If there is some other kind of coupling present (e.g., the magnetic dipole interaction), it will have to bear the same ratio (which is not probable), or else it must be negligibly small.

Figure 14 shows a comparison between the calculated and experimental spectra for the $J=0\rightarrow 1(K=0)$ transition of CH_3Cl^{35} before and after Zeeman splitting. Calculations were performed by putting the known quantities $I(Cl^{35})=3/2$, $g(Cl^{35})=0.547$ and $H=1670$ oersteds (experimental) into Eq. (13) to see what value of g_{mole} will best fit the experimental pattern. This amounts to an experimental determination of $g_{mole}(CH_3Cl^{35})$, which is the only unknown factor. It turns out that the best fit occurs when we assume $g_{mole}\ll g_N(Cl^{35})$. While it is not possible to observe experimentally all the theoretical Zeeman components because of insufficient resolution and sensitivity, the general agreement seems to be good. This may be taken as further evidence supporting the general theory developed in Section C of Part III.

G. Zeeman Effect of SO_2

Since SO_2 has no known nuclear magnetic moment, the only contribution toward the Zeeman effect should come from its molecular moment. This molecule is different from $N^{15}H_3$ in that it is an asymmetric top and it has a larger reduced mass. The Zeeman effect of such a molecule has been investigated at the known frequencies published by Dailey and others.[18] It turned out, at $H=1670$ oersteds, that all the lines tested showed an incipient Zeeman effect in the form of a very marked reduction of the line intensity and accompanying broadening of the line. The splitting is, however, in no case resolvable in this weak field. It is hoped that complete resolution can be achieved with a stronger field. These results will be interesting from the standpoint of the size of the molecular g-factor and also as an aid to the assignment of quantum numbers to the spectral lines through the individual characteristics of the Zeeman patterns.

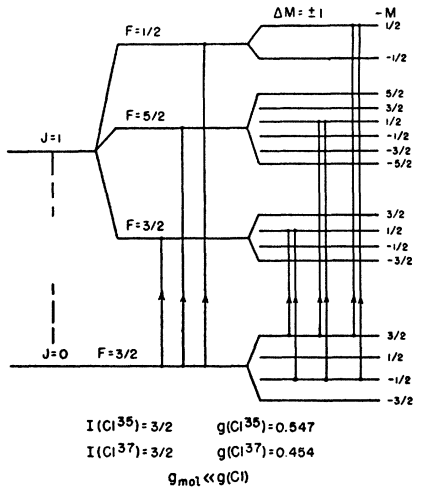

FIG. 13. Energy level diagram and Zeeman splitting for CH_3Cl.

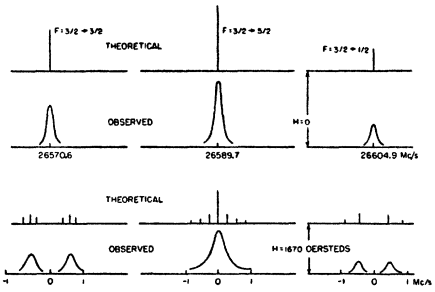

FIG. 14. The $J=0\rightarrow 1$ lines of CH_3Cl^{35} with and without magnetic field, $I(Cl^{35})=\frac{3}{2}$, $g(Cl^{35})=0.547$, $g_{mole}\ll g_N(Cl^{35})$.

[16] W. Gordy, J. W. Simmons, and A. G. Smith, Phys. Rev. **72**, 344 (1947).
[17] C. H. Townes, A. N. Holden, J. Bardeen, and F. R. Merritt, Phys. Rev. **71**, 644 (1947).
[18] B. P. Dailey, S. Golden and E. B. Wilson, Jr., Phys. Rev. **72**, 871 (1947).

IV. CONCLUSION

From the above preliminary studies on the Zeeman effect in the absorption spectra of gas molecules, it is seen that a knowledge of the nuclear and molecular g-factors can be obtained from the analysis of Zeeman splitting, if there exists a spin-rotation coupling. If one g-factor is known, the other g-factor can be determined from the experimental data, on the basis of known spin and rotational quantum numbers. By studying the Paschen-Back effect at strong fields in conjunction with the analysis of the Zeeman effect, it will be possible to evaluate the two g-factors separately.

If the spin-rotation coupling is absent, the Zeeman splitting of the spectral lines of a molecule will yield direct information on the molecular g-factor. This information bears a close relationship to the charge distribution in a molecule and may throw some light on the nature of molecular bonds. The same knowledge should be particularly useful for the study of the interaction between the nuclear magnetic moment and the magnetic moment resulting from molecular rotation. Also, if the spectral lines of a molecule differ among themselves in their characteristic Zeeman patterns, the Zeeman studies can lend much help to the identification and assignment of molecular lines.

A new magnet-cavity assembly has now been built which is capable of yielding a magnetic field of the order of 10,000 oersteds. It is planned that more intensive investigations will be carried out for a large class of molecules in both the Zeeman and Paschen-Back spectra.

ACKNOWLEDGMENTS

I am deeply indebted in this work to Professor E. L. Chaffee for much encouragement, Mr. S. P. Cooke for technical advice, and Professors J. H. Van Vleck and E. B. Wilson, Jr. for very valuable suggestions.

PHYSICAL REVIEW VOLUME 74, NUMBER 10 NOVEMBER 15, 1948

Relation between Apparent Shapes of Monoenergetic Conversion Lines and of Continuous β-Spectra in a Magnetic Spectrometer*

G. E. OWEN AND H. PRIMAKOFF
Department of Physics, Washington University, St. Louis, Missouri

(Received August 2, 1948)

A method has been worked out for correcting distortions which affect the apparent shape of a continuous β-ray spectrum. Internal conversion lines are studied in the β-spectrometer and found to have a finite width and in the case of 180° focusing an unsymmetrical shape.

On the assumption that these conversion lines are actually monoenergetic, it is possible to calculate the distortion produced by the spectrometer and source, and thus to determine the approximate true shape of the continuous β-ray spectrum from the experimental data.

The Kurie plots for a continuous β-ray spectrum corrected in this way are, in general, straight over a greater range than the plots of the uncorrected data. The correction has been applied to the ratio of the number of positrons to the number of negatrons in Cu^{64} and gives results in better agreement with the Fermi theory than if there has been no correction.

1. INTRODUCTION

IN recent years one of the most important problems in the investigation of the shapes of the continuous β-spectra has been the study of their low energy regions. In the course of such study, discrepancies have been reported between experiment and the Fermi theory, in particular, for the supposedly allowed β^+- and β^--spectra from Cu^{64}.[1] In the present note, a systematic method is described for correcting

* Assisted by the joint program of the Office of Naval Research and Atomic Energy Commission.

[1] C. S. Cook and L. M. Langer, Phys. Rev. **73**, 601 (1948); J. Backus, Phys. Rev. **68**, 59 (1945).

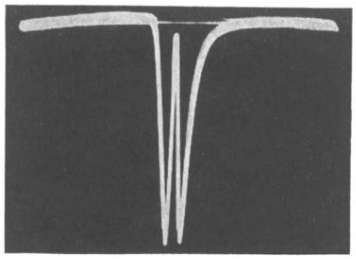

FIG. 3. Oscilloscopic pattern for a spectral line in cavity resonance.

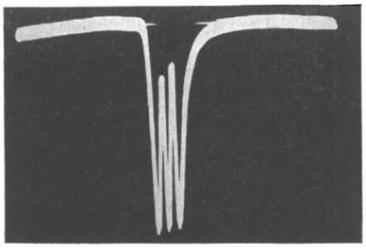

FIG. 4. Zeeman splitting of a spectral line in cavity resonance at $H = 700$ oersteds.

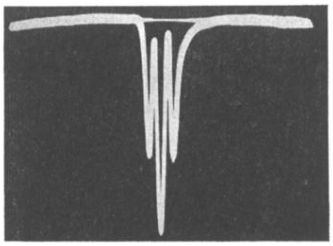

FIG. 5. Zeeman splitting of a spectral line in cavity resonance at $H = 1200$ oersteds.